# Hierarchical brain mapping via a generalized Dirichlet solution for mapping brain manifolds *

Sarang C. Joshi , Michael I. Miller,

Department of Electrical Engineering and Inst. for Biomedical Computing
Washington Univ., St. Louis, MO 63130.

Gary E. Christensen,

Department of Surgery and Mallinckrodt Institute of Radiology,
Washington Univ. School of Medicine, St. Louis, MO 63110.

Ayananshu Banerjee,

Department of Electrical Engineering, Washington Univ., St. Louis, MO 63130.

Tom Coogan,

Department of Anatomy and Neurobiology,
Washington Univ. School of Medicine, St. Louis, MO 63110.

and Ulf Grenander

Division of Applied Mathematics, Brown Univ., Providence, RI 02912

## ABSTRACT

In this paper we present a *coarse-to-fine* approach for the transformation of digital anatomical textbooks from the *ideal* to the *individual* that unifies the work on landmark deformations and volume based transformation. The Hierarchical approach is linked to the Biological problem itself, coming out of the various kinds of information which is provided by the anatomists. This information is in the form of points, lines, surfaces and sub-volumes corresponding to 0,1,2 and 3 dimensional sub-manifolds respectively. The algorithm is driven by these sub-manifolds. We follow the approach that the highest dimensional transformation is a result from the solution of a sequence of lower dimensional problems driven by successive refinements or partitions of the images into various Biologically meaningful sub-structures.

*This work was supported by NIH grants RR01380 and RO1-MH52158-01A1 and ARO DAAL-03-86-K-0110

# 1 Introduction

We have been studying the variability of human and macaque anatomy by generating smooth maps from a single template to a family of targets.[1–5] In our approach the template represents the typical structure; variation is accommodated by the definition of probabilistic transformations applied to the templates. The transformations form groups (translation, scale, and rotation), globally applied (rigid) for registration and locally applied for fine detailed shape deformation. The transformations on which we focus are defined by vector fields $u(\cdot)$, applied throughout the coordinate system of the template (defined as $\Omega$), thereby accommodating a very fine variation in anatomy: $x = (x_1, x_2, x_3) \in \Omega \mapsto (x_1 - u_1(x), x_2 - u_2(x), x_3 - u_3(x)) \in \Omega$. The maps constructed from these high dimensional vector field transformations allow for the dilation, contraction, and warping of the underlying ideal coordinates of the template into the coordinates of the individual anatomy.

Herein, we concentrate on whole brain volumes generated via CRYOSECTION imaging. The *target* is analyzed by constructing the transformation which carries the coordinate systems of the template into the target, with the driving function for the registration forced by a distance measure $D(u)$ between the transformed textbook and the target. The distance measures used are derived from the physics of the sensing modality; we have predominantly used Gaussian distance measures between the deformed template and the data (see[1] for example).

As the transformation from the template to the target is used to study geometric properties, the transformation must be smooth so that connected sets remain connected, surfaces are mapped as surfaces, and the global relationships between structures are maintained. To enforce smoothness properties on the transformation, the transformations are forced to arise from a prior probability distribution with energetics $E(u)$ reflecting the kinematics associated with elastic and fluid media.[1,5,2,3] The introduction of the prior distribution places our solution in the class of *Bayesian inference problems*, that of inferring the transformation of the template minimizing both the distance measure $D(u)$ and the potential energy $E(u)$ of the prior distribution.

The 3-D whole brain maps correspond to the Bayesian maximizer, whose variational solution corresponds to a solution of a non-linear PDE, consisting of between $10^7 - 10^8$ parameters in the vector field on the whole 3-D lattice. We believe that there should be a *coarse-to-fine* principal in ultimately deriving the full vector field, the coarse to fine driven by the Biological problem itself. We have been building such a procedure based on information which is provided by the anatomists themselves about the various substructures of the brain, and varying degrees of knowledge about these substructures. In what we now develop, this will imply that the brain mapping algorithm will be driven by subsets of defined points, lines, surfaces and or predefined volumes that serve as preconditioning or input to the ultimate Bayesian solution of the PDE on the full continuum. Our motivation is to follow the approach that the highest dimensional transformation will ultimately be completely driven by the 3-dimensional imaging data alone. However, lower dimensional information input by the anatomists will provide efficient preconditioning to the final solution, and will result in the full solution via a solution of a sequence of lower dimensional problems driven by successive refinements or partitions of the images into the Biologically meaningful sub-information. This approach unifies the elegant work of Bookstein on landmark deformations and the volume based transformation work described by various authors.[1,2,5,3,6,7]

As the prior distribution is the glue which unifies our hierarchical approach it will play an important role in our formulation, we therefore briefly summarize its construction.

# 2 Mathematical construction of the Gaussian prior

Begin with a brain volume defined on the domain $\Omega = [0,1]^3 \subset \Re^3$, the unit cube. The prior distribution is induced by defining the transformation fields $\{u(x), x \in \Omega\}$, to satisfy stochastic partial differential equations of the type $L\ u(x) = e(x)$, $x \in \Omega$, $L$ a local (bounded support) self-adjoint positive differential operator.

Randomness enters into the prior through $e(x)$ a $3 \times 1$ white Gaussian random field. In all of our previous work we have used operators induced by continuum mechanics corresponding to elasticity[1,5,3,4] and fluid operators.[5,2]

We shall focus on the elasticity operators herein, in which case $L = a\nabla^2 + b\nabla\nabla\cdot + cI$. $\nabla^2$ and $\nabla$ are the Laplacian and divergence operators $\frac{\partial^2}{\partial x_1} + \frac{\partial^2}{\partial x_2} + \frac{\partial^2}{\partial x_3}$, $\nabla = [\frac{\partial}{\partial x_1}, \frac{\partial}{\partial x_2}, \frac{\partial}{\partial x_3}]^T$, and $a$, $b$ and $c$ are constants. As $L$ is a linear operator, this induces Gaussian random fields (see,[8] for example) as follows.

PROPOSITION 1. *Let $L$ be a constant coefficient local (bounded support),positive (invertible) differential operator, and let $\{u(x), x \in \Omega\}$ be a random process satisfying*

$$Lu(x) = e(x) \tag{1}$$

*where $e(x)$ is white noise. Then $\{u(x), x \in \Omega\}$ is a zero-mean Gaussian process with covariance*

$$K(x,y) = \int G(x,u)G(y,u)du \ ,$$

*where $G$ is the Green's function of $L$ satisfying $LG(x,y) = \delta(x-y)$.*

*Proof:* Let $e_f = \int e(x)f(x)dx$, $f \in \mathcal{S}$ the family of test functions. By definition of $u$ in Eqn. 1

$$e_f = \int Lu(x)f(x)dx = \int u(x)L^\dagger f(x)dx \ ,$$

$(\cdot)^\dagger$ denoting the adjoint. As $e(x)$ is white noise, $e_f$ is zero-mean with variance $< f, f >$. Let $K_u$ be the covariance operator of $u$, then by definition of the covariance operator of a Gaussian field (Kuo[9] pg. 15), for all $f \in \mathcal{S}$,

$$\begin{aligned} < f, f > &= < L^\dagger f, K_u L^\dagger f > \\ &= < f, LK_u L^\dagger f > \end{aligned}$$

implying $LK_uL^\dagger = I$. Now as the covariance is a positive operator by the square root lemma[10] we can write $K_u = GG^\dagger$, and with $G$ defined to be a positive operator gives $LG(x,y) = \delta(x-y)$, where the *dirac delta* function $\delta(x-y)$ is interpreted as the identity operator. □

# 3 A Hierarchical Solution Via The Generalized Dirichlet Mapping of Brain Manifolds

The hierarchical approach is fundamentally driven by the Biological problem itself. The procedure is based on information provided by the anatomists themselves about the various substructures of the brain, and varying degrees of knowledge about these substructures. The information will correspond to easily identifiable points, lines, surfaces and subvolumes in the target corresponding to landmarks, sulcal lines, cortical surfaces, and major nuclei. These points, lines, surfaces, and subvolumes are examples of 0,1,2,3 dimensional manifolds and will initially constrain the transformation from one brain to the other.

As we show below, the idea of constraining the maps via manifolds can be viewed as the solution of a *generalized Dirichlet problem*. Our strategy will be to solve the *Dirichlet problem* associated with elastically extending the transformation from the various easily identifiable components to the full volume continuum. This provides a "coarse registration", and is the initial step in our brain deformation process. Its only purpose is to act as a preconditioning of the final mapping solution based on the full PDE formulation.

We begin by assuming that $\Omega$ can be written as a disjoint partition $\Omega = \cup_{i=0}^{i=3}\mathcal{M}(i), \mathcal{M}(i)$ an $i$ = 0,1,2, or 3 dimensional manifolds constituting the various Biologically meaningful sub-structures. To illustrate examples of

manifolds, shown in Figure 1 are renderings corresponding to the 3-D whole brain volumes of a macaque consisting of the $640 \times 480 \times 200$ voxel volume (left panel). Superimposed over the rendering are the observable sulcal maps sitting on the pial surface of the whole brain. The middle panel shows a $C^2$ manifold representing the cortical surface. The right panel shows a slice through a whole brain cryosection with the cortical surface embedded in the volume delineating the interface between the gray and the white matter.

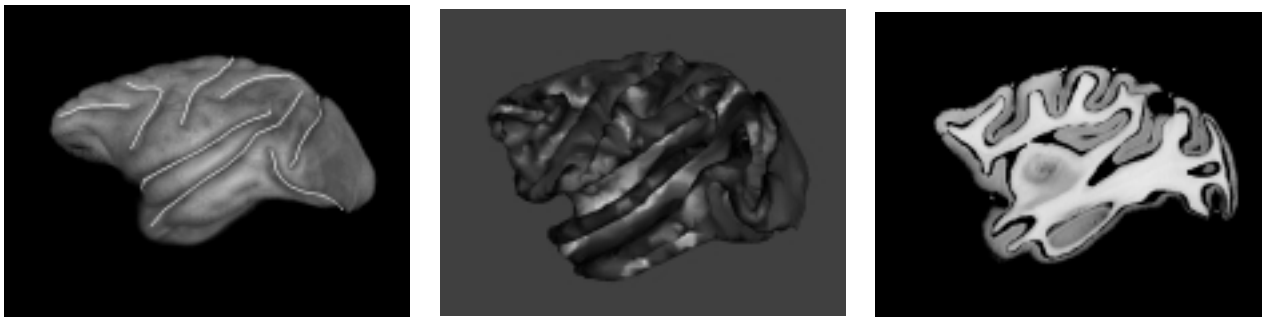

Figure 1: SULCAL PATTERN EXTRACTION. Left panel shows a whole macaque brain with the sulci depicted. The middle panel shows the $C^2$ manifold representing the cortical surface. The right panel shows a slice through a whole brain cryosection with the cortical surface embedded in the volume delineating the interface between the gray and the white matter.

Considering a subset of manifolds as predetermined, or given with perfect resolution, gives us the notion of *observable manifolds*.

DEFINITION 3.1. *A manifold $\mathcal{M} \in \Omega$ of dimension $m = 0,1$ or 2 is called an observable manifold if its map in the observed data can be identified exactly.*

We use this concept to condition the prior distribution, that is assume we are given the observable manifolds $\mathcal{M}(i)$ along with the vector field on the manifold i.e. $u(x) = k(x), x \in \mathcal{M}(i)$ mapping the observable manifolds in the template to the data. Such observable manifolds will most naturally correspond to fiducial landmarks (0-dimensional points) and sulcal maps (1-dimensional lines), cortical surfaces (2-dimensional) and major nuclei (3-dimensional subvolumes). The equality constrained Bayesian problem becomes the following.

*Problem Statement:* The Bayesian equality constrained problem becomes

$$\text{Minimize} \quad \int_\Omega |Lu(x)|^2 dx \quad \text{subject to } u(x) = k(x) \ , \ x \in \bigcup_{i=0}^{3} \mathcal{M}(i) \ . \tag{2}$$

## 3.1 The Generalized Dirichlet Problem

PROPOSITION 2. *Let $\mathcal{M}$ be a smooth manifold and $L$ self adjoint. Then the minimizer of the functional*

$$F(u) = \int_\Omega |Lu(x)|^2 dx \quad \text{subject to } u(x) = k(x) \ , \ x \in \mathcal{M} \tag{3}$$

*is unique satisfying $L^2 \hat{u}(x) = 0$, $\forall x \in \Omega \setminus \mathcal{M}$, with the solution written in the form of a Fredholm integral equation*

$$\hat{u}(x) = \int_{\mathcal{M}} K(x,y)\beta(y) dS(y) \ , \tag{4}$$

*where $K = GG^{\dagger}$ and $G$ the Green's function of $L$, and $dS$ the Hausdorff measure on the manifold.*

*Proof:* Using the usual definition of the Gateaux differential (pg. 171 of[11]) of the functional $F$ gives

$$\delta F(u;\eta) = \lim_{\epsilon \to 0} \frac{F(u+\epsilon\eta) - F(u)}{\epsilon}|_{\epsilon=0} \quad (5)$$

$$= \int_{\Omega} \eta(x)\, L^2 u(x) dx \ . \quad (6)$$

Here we have used the fact that the operator $L$ is self-adjoint. A necessary condition for the minimizer is that the Gateaux differential $\delta F(u)$ is zero for all allowable perturbations $\eta$. This implies that if $\hat{u}$ is a minimizer of Eqn. 3 then

$$L^2 \hat{u} = 0 \ \text{ subject to } u(x) = k(x) \ , \ x \in \mathcal{M} \ .$$

This is the *Dirichlet* problem and has a unique Fredholm solution given by Eqn. 4 (see Reed and Simon[10] Pg. 204-206). □

There are several special cases of interest when the observable manifolds $\mathcal{M}$ are surfaces (cortical folds), lines (sulci), and points (landmarks). We can now state the Bayesian problem and the solution associated with each of the cases.

1. **Surface manifolds.** When the observable manifold in Eqn. 2 is a 2-dimensional closed surface the problem is the *classical Dirichlet Problem.* To see this, let $\mathcal{M}(2)$ be a smooth 2-dimensional closed surface. Then the *Bayesian estimator*,

$$\hat{u} = \arg\min\{u\} \int_{\Omega} |Lu(x)|^2 dx \ \text{ subject to } u(x) = k(x) \ , \ x \in \mathcal{M}(2) \ , \quad (7)$$

   is unique satisfying $L^2\hat{u}(x) = 0$, $\forall x \in \Omega \setminus \mathcal{M}(2)$; the solution given by a Fredholm integral equation,

$$\hat{u}(x) = \int_{\mathcal{M}(2)} K(x,y)\beta(y) dS(y) \ ,$$

   with $K = GG$ and $G$ the Green's function of $L$, and $dS$ the surface measure.

2. **Linear manifolds (sulci).** For considering manifolds which are *lines*, $\mathcal{M}(1)$ , we need only change the surface measure to line measures. Given equality constraints $u(x) = k(x), x \in \mathcal{M}(1)$ associated with a collection of 1-dimensional linear manifolds $\mathcal{M}(1)$, the solution can be written in form of a Fredholm integral equation given by

$$\hat{u}(x) = \int_{\mathcal{M}(1)} K(x,y)\beta(y) dl(y) \ ,$$

   with $dl$ the line measure on $\mathcal{M}(1)$.

3. **Point manifolds (landmarks).** For considering manifolds which are *points* ,$\mathcal{M}(0)$, we need only change the surface measure to atomic measures. The 0-dimensional manifold work is of course directly analogous to what has emerged from the work of Bookstein[12,13] on landmark-based deformations. In fact, for the landmarks (points) , the solution can be computed in closed form by a solution of $N$ linear equations.[14,15] Given the equality constraints associated with the collection of $N$-points $u(x) = k(x), x \in \mathcal{M}(0) = \bigcup_{i=1}^{N} x_i$, the minimizer $\hat{u}$ is unique and satisfies $N$-linear equations

$$\hat{u}(x) = \sum_{i=1}^{N} \beta_i K(x, x_i) \ .$$

   Our proof follows the clear exposition of Kent[14] on Kriging methods.

COROLLARY 1. *Given the equality constraints associated with the collection of $N$-points $u(x) = k(x), x \in \mathcal{M}(0) = \bigcup_{i=1}^{N} x_i$, the minimizer $\hat{u}$ is unique and satisfies $N$-linear equations*

$$\hat{u}(x) = \sum_{i=1}^{N} \beta_i K(x, x_i) \ , \tag{8}$$

*where $\beta_1, \cdots, \beta_N$ satisfies the system of linear equations*

$$\begin{bmatrix} K(x_1,x_1) & K(x_1,x_2) & \cdots & K(x_1,x_N) \\ K(x_2,x_1) & K(x_2,x_2) & \cdots & K(x_2,x_N) \\ \vdots & \vdots & \vdots & \vdots \\ K(x_N,x_1) & K(x_N,x_2) & \cdots & K(x_N,x_N) \end{bmatrix} \begin{bmatrix} \beta_1 \\ \beta_2 \\ \vdots \\ \beta_N \end{bmatrix} = \begin{bmatrix} k_1 \\ k_2 \\ \vdots \\ k_N \end{bmatrix} \ , \tag{9}$$

*and $K$ is the covariance determined by the Green's operator squared, $K(x,y) = \int_\Omega G(x,s)G(y,s)ds$.*

*Proof:* Let $\hat{u}$ be as defined in Eqn. 8, then any function $f(x)$ satisfying the constraints becomes

$$\begin{aligned} f(x) &= \hat{u}(x) + \rho(x) \\ &= \sum_{i=1}^{N} \beta_i K(x, x_i) + \rho(x) \end{aligned}$$

where $\rho(x_i) = 0, i = 1, \cdots N$. Then

$$\int_\Omega |Lf(x)|^2 dx = \int_\Omega |L[\sum_{i=1}^{N} \beta_i K(x, x_i)]|^2 + |L\rho(x)|^2 dx + 2\sum_{i=1}^{N} \beta_i \int_\Omega LK(x, x_i) L^\dagger \rho(x) dx \ .$$

But

$$\begin{aligned} \int_\Omega L(\int_\Omega G(x_i,t)G(x,t)dt)L^\dagger \rho(x)dx &= \int_\Omega L(G(x_i,x)\rho(x))dx \\ &= \rho(x_i) = 0 \ , \end{aligned}$$

implying

$$\begin{aligned} \int_\Omega |Lf(x)|^2 dx &= \int_\Omega |L[\sum_{i=1}^{N} \beta_i K(x, x_i)]|^2 + |L\rho(x)|^2 dx \\ &= \int_\Omega |L\hat{u}(x)|^2 dx + |L\rho(x)|^2 dx \ . \end{aligned}$$

Thus for all $f$ satisfying the constraints

$$\int_\Omega |Lf(x)|^2 dx \geq \int_\Omega |L\hat{u}(x)|^2 dx \ .$$

□

Now let us suppose that the manifolds are collections of points and are not fully observable in the data but there are errors associated with the observation process. Assume Gaussian noise around the observations.

DEFINITION 3.2. *A noisy observable manifold of $N$-points $\mathcal{M}(0) = \cup_{i=1}^{N} x_i$ is one which can be identified to within a random neighborhood of Gaussian radius with variance $\sigma^2$.*

We assume that errors are independent and Gaussian distributed with zero mean and variance $\sigma^2$. Then the Bayesian problem and solution becomes:

COROLLARY 2. *Given noisy observable points $k_i = u(x_i) + n(x_i), i = 1 \ldots N$, $n(x_i)$ are Gaussian distributed with variance $\sigma^2$, the minimizer of*

$$\hat{u} = \arg\min_u \int_\Omega |Lu|^2 + \sum_{i=1}^{N} \frac{|k_i - u(x_i)|^2}{\sigma^2} \tag{10}$$

*satisfies*

$$\hat{u}(x) = \sum_{i=1}^{N} \beta_i K(x, x_i)$$

*where $\beta = [\beta_1, \cdots, \beta_N]^t$ satisfy the system of linear equations*

$$(K + \sigma^2 I)\beta \quad = \quad \mathbf{k}$$

*with $\mathbf{k} = [k_1, \cdots, k_N]^t$, and $K, I$ are $N \times N$ matrices with $K(i,j) = K(x_i, x_j)$ and $I$ the identity matrix.*

*Proof:* We first note that if $u(x_i)$ are fixed then the optimal solution is given by Theorem 2. Hence we can restate the problem as finding $\beta$ which minimize

$$\frac{1}{\sigma^2}|\mathbf{k} - K\beta|^2 + \beta^t K \beta \ .$$

The solution to this is readily found to be $\beta$ that satisfy system of linear equations

$$(K + \sigma^2 I)\beta \quad = \quad \mathbf{k} \ .$$

□

Note above that the matrix $K$ is invertible as it is a covariance matrix of the Gaussian process defined in Section 2.

# 4 Coarse-to-fine mapping via a basis solution of the PDE.

The solution of the Dirichlet problem based on the observable manifolds represents the coarse step in the transformation. Having completed the coarse step in the transformation, the volumes are roughly aligned and attention can now be focused on the fine featured substructures. The second step is to solve the registration problem using the full volume data. The cryosection volume data is the only information on which this part of the algorithm runs. The sulcal maps play only the role of providing an initial alignment at the coarsest level.

## 4.1 Bayesian estimation of the transformation

The Bayesian *maximum a-posteriori* (MAP) estimator solving the final registration problem is the transformation satisfying the maximization

$$\hat{u} = \arg\max_u(-D(u) - E(u)) \ , \tag{11}$$

where $D(u)$ is the distance measure between the transformed textbook and the target and $E(u)$ is the energetics of the prior probability distribution reflecting the kinematics associated with elastic media. The distance measures

used are derived from the physics of the sensing modality; we have predominantly used Gaussian distance measures between the deformed template and the data. The maximization in Eqn 11 is conditioned using the information provided by the anatomists about the various substructures by writing the deformation field as a refinement of the Dirichlet solution associated with the various observable sub-manifolds. Let $u_{\mathcal{M}}$ be the solution of the Dirichlet problem associated the with sub-manifolds $\mathcal{M}$. We write the deformation as

$$u(x) = u_{\mathcal{M}}(x) + u_1(x)$$

where $u_1$ is the refinement of the Dirichlet solution. The MAP estimator is the variational calculus maximizer $\hat{u}$ corresponding to partial differential equations (PDE's) defined on the continuua. For linear elastic solids the stress or restoring force grows proportionately to the strain or deformation distance away from the template. The resulting PDE which the MAP estimator $\hat{u}$ satisfies for a linear elastic solid is given by

$$\mu\nabla^2 u(x) + (\lambda + \mu)\nabla(\nabla \cdot u(x)) = b(x - u(x)) \ , \tag{12}$$

where the distributed body force $b(x - u(x)) = \nabla_u D(u)$ is the gradient of the registration distance (See[1,5,2] for details). A coarse to fine approach is used in solving the elasticity based PDE, Eqn. 12, on the full volume as follows. The vector field $u_1(\cdot)$ defined on $\Omega = [0, 1]^3$ is written using a complete orthonormal basis expansion. Define

$$u(x) = \sum_{k=0}^{\infty} \mu_k \phi_k(x) + \sum_{i=1}^{N} \beta_i K(x, x_i) \tag{13}$$

where the basis $\{\phi\}$ corresponds to the eigenfunctions of the elasticity operator $L = a\nabla^2 u(x) + b\nabla\nabla\cdot$, derived in[2,5] and the second term is the solution to the Dirichlet problem derived in section 3. The optimization is accomplished by solving a sequence of optimization problems from coarse to fine scale via parametrically defined deformation fields. This is analogous to multi-grid methods but here the notion of refinement from coarse to fine is accomplished by increasing the number of basis components. The iterations are started with the solution of the Dirichlet problem and then the eigenfunctions are incrementally added. As the number of basis functions is increased, smaller and smaller variabilities between the textbook and target are accommodated.

# 5 Results

Examine the whole macaque cryosection brains ($500^2 \times 200$ voxels) shown in Fig. 1 in which the gyri and associated sulci have been labeled in David Van Essen's laboratory in the Department of Anatomy and Neurobiology at Washington University. We have defined sulci as piecewise linear curves. We have done this in several whole brains following the nomenclature used in Felleman and Van Essen.[16] The sulcal maps constrain the transformation from one brain to the other. In Fig. 1 each of the sulci have been identified and placed into the whole brains discretized to 16 points in each of the brains. The deformation field was constrained so that the corresponding points where mapped on to each other involving roughly 200 parameters total to represent the solution based on mapping the sulci.

To accommodate the global rigid motion between the two brain we add the affine group. Define the vector field transformations $x \mapsto x + Ax + \vec{a} - u(x)$, where $A$ represents $GL(3)$ , $\vec{a}$ the translation and $u(x) = [u_1(x), u_2(x), u_3(x)]$, with energetics $E(u) = \int |Lu(x)|^2 dx$ and the Laplacian operator $L = \nabla^2 + bI$. Then $\{u(x), x \in \Omega\}$ is a vector valued Gaussian field over $\Omega$ defined by the covariance

$$K_u(x, y) = \begin{bmatrix} K(x, y) & 0 & 0 \\ 0 & K(x, y) & 0 \\ 0 & 0 & K(x, y) \end{bmatrix} \ ,$$

with the covariance given by the squared Green's function, implying $K(x, y) = e^{-b|x-y|}$.

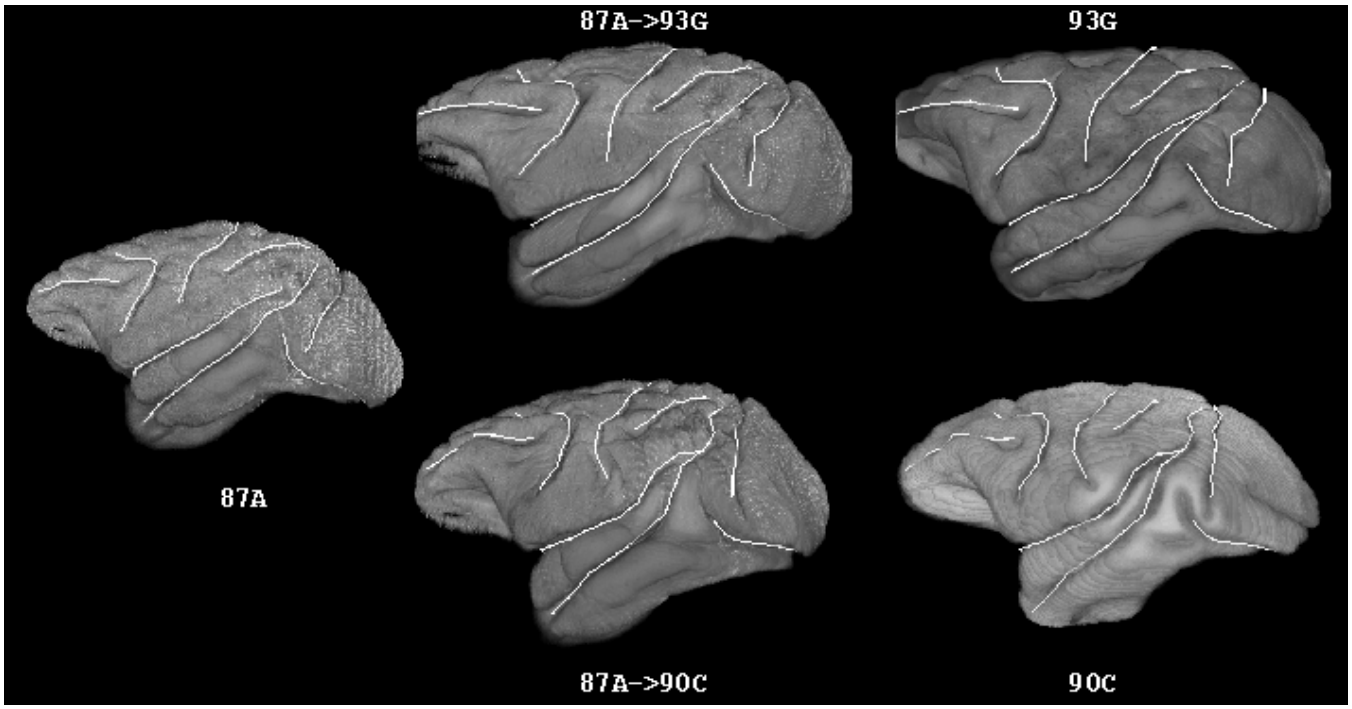


Figure 2: The left panel shows the template 87A. The middle shows the the transformed templates with the deformation driven only by the sulcal maps. The right panel shows two targets 93G and 90C and their sulcal maps.

The *Bayesian estimator* becomes

$$\hat{u} = \arg\min_{\{u\}} \sum_{i=1}^{3} \int_{\Omega} |\nabla^2 u_i(x) + b u_i(x)|^2 dx \quad \text{subject to} \quad u(x) = k(x) \quad x \in \{\cup_{i=1}^{N} x_i\} \ .$$

The optimum deformation field becomes

$$\hat{u}(x) = \sum_{i=0}^{N} K_u(x, x_i)\vec{\beta}_i$$

where $\vec{\beta}_i = [\beta_1, \beta_2, \beta_3]$ satisfies the system of Equations 9.

Figure 2 is the volume rendering of the template 87A (left panel) and the template mapped to the targets (middle panel) using only the sulcal line constraints to define the transformation. The right panel shows the target brains 90C and 93G. Figure 3 shows corresponding slices through the template 87A (left) the target 93G (right) and the deformed template (middle). Notice that there is a large difference in the shape and positions of the major subvolumes (the thalamus and the cortical folds) between the undeformed template and the target. Notice the improvement in the alignment of the major subvolumes in the deformed template with the target after the sulcal map deformation.

The transformation was further refined by solving the the elasticity based PDE, Eqn. 12, on the full volume using the procedure outlined in section 4. Figure 4 demonstrates the hierarchical procedure. The figure shows slices through the template volume 87A and the corresponding slices through the deformed template at the different levels of the hierarchy. Column two shows the result based on the sulcal map constraints. Column three shows the result after the solution of the PDE. The target 93G is shown on the right.

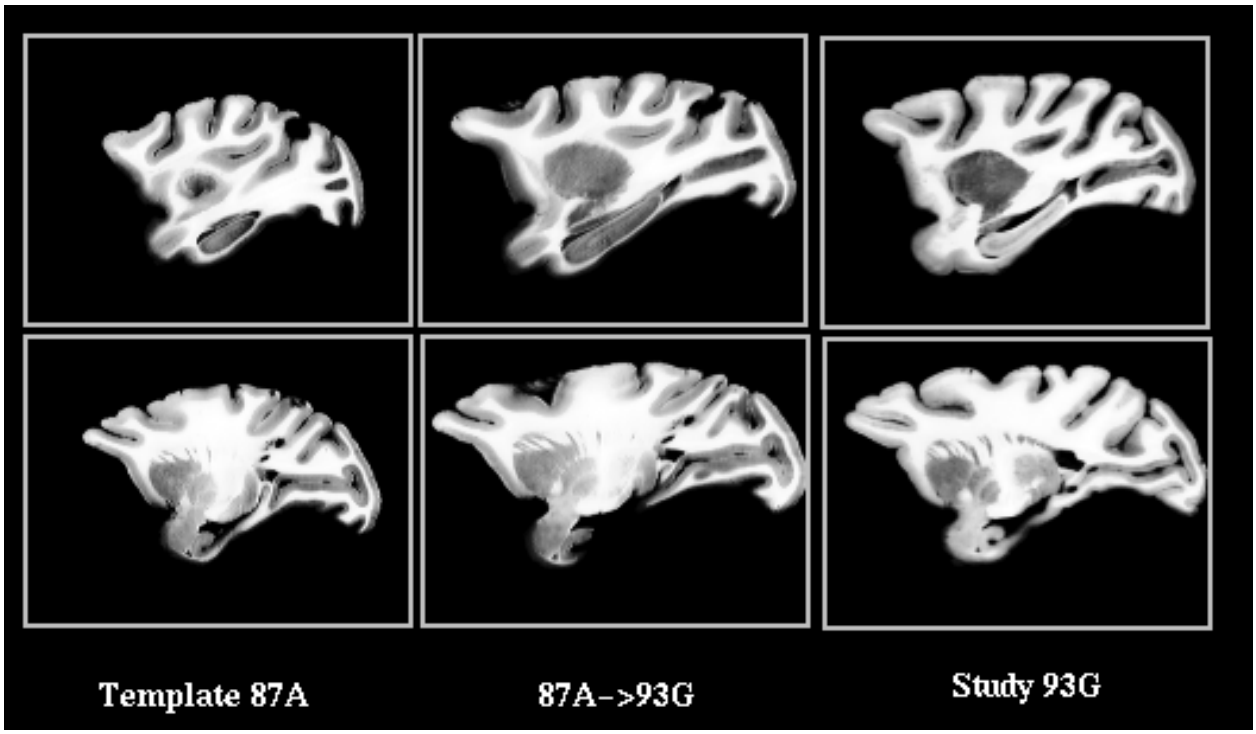


Figure 3: The left panel shows slices through the template 87A and the corresponding slices through the deformed template (middle) and the target 93G (right). Notice the improvement in the alignment of the major subvolumes after the sulcal map deformation.

The flow of coarse to fine information is depicted in Figure 5. The left panel shows the large differences before any transformation has been applied. The middle panel shows the correspondence after the solution of the Dirichlet problem associated with constraining the sulcal maps. The right panel shows the correspondence after the application of the parametrically defined, basis transformation. Notice, the local transformation associated with the PDE allow for small adjustments of the fine featured substructures.

## 6 Acknowledgments

We are indebted to Dr. Van Essen for the Cryosection data and Michael Vannier for helpful discussions during the development of the manuscript. This work was supported by NIH grants RR01380 and RO1-MH52158-01A1 and ARO DAAL-03-86-K-0110.

## 7 REFERENCES

[1] M.I. Miller, G.E. Christensen, Y. Amit, and U. Grenander, "Mathematical textbook of deformable neuroanatomies", *Proceedings of the National Academy of Science*, vol. 90, no. 24, Dec. 1993.

[2] G. E. Christensen, R. D. Rabbitt, and M.I. Miller, "3D brain mapping using a deformable neuroanatomy", *Physics in Medicine and Biology*, vol. 39, pp. 609–618, 1994.

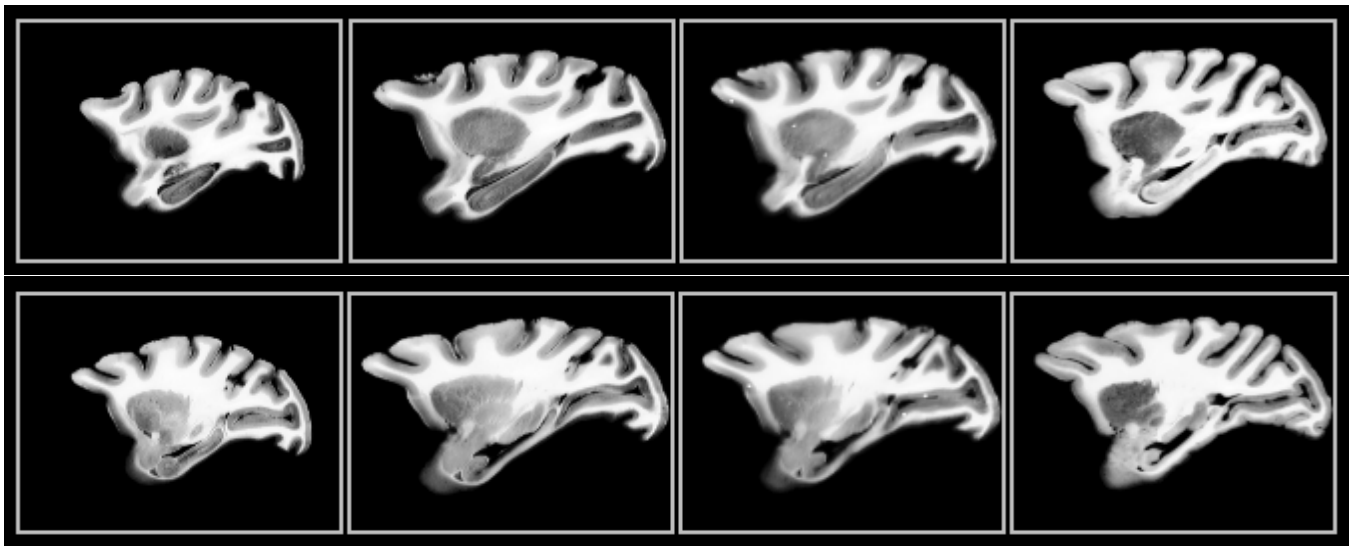

Figure 4: The left column shows slices through the template volume 87A and the corresponding slice through the deformed template at the different levels of the hierarchy (columns 2 and 3) and the target 93G (right). Notice the improving alignment of the major subvolumes after the manifold based transformation (column 2) and the refinement by the volume based transformation (column 3).


[3] U. Grenander and M. I. Miller, "Representations of knowledge in complex systems", *Journal of the Royal Statistical Society B*, vol. 56, no. 3, pp. 549–603, 1994.

[4] M. W. Vannier, M. I. Miller, and U. Grenander, "Modeling and data structure for registration to a brain atlas of multimodality images", in *Functional Neuroimaging- Technical Foundations*, edited by R. W. Thatcher, M. Hallett, T. Zeffiro, E. R. John, and M. Huerta, Eds., pp. 217–221. Academic Press, 1994.

[5] G. Christensen, *Deformable Shape Models for Anatomy*, Ph.D. Thesis, Department of Electrical Engineering, Sever Institute of Technology, Washington University, St. Louis,MO, August 1994.

[6] A.C. Evans, W. Dai, L. Collins, P. Neelin, and S. Marret, "Warping of a computerized 3-d atlas to match brain image volumes for quantitative neuroanatomical and functional analysis", *Image Processing*, vol. 1445, pp. 236–246, 1991.

[7] Y. Amit, U. Grenander, and M. Piccioni, "Structural image restoration through deformable templates", *J. American Statistical Association*, vol. 86, no. 414, pp. 376–387, June 1991.

[8] Y. Amit and M. Piccioni, "A nonhomogenous markov process for the estimation of gaussian random fields with non-linear observations", *The Annals of Probability*, vol. 19, pp. 1664–1678, 1991.

[9] Hui-Hsiung Kuo, *Gaussian Measures in Banach Spaces*, vol. Lecture Notes in Mathematics - 463, Springer-Verlag, 1975.

[10] M. Reed and B. Simon, *Functional Analysis I: Revised and Enlarged Edition*, Academic Press, 1980.

[11] D.G. Luenberger, *Optimization by Vector Space Methods*, John Wiley and Sons, New York, 1969.

[12] F.L. Bookstein, *The Measurement of Biological Shape and Shape Change*, vol. 24, Springer-Verlag: Lecture Notes in Biomathematics, New York, 1978.

[13] F.L. Bookstein and W.D.K. Green, "Edge information at landmarks in medical images", in *Visualization in Biomedical Computing 1992*, Richard A. Robb, Ed. 1992, pp. 242–258, SPIE 1808.

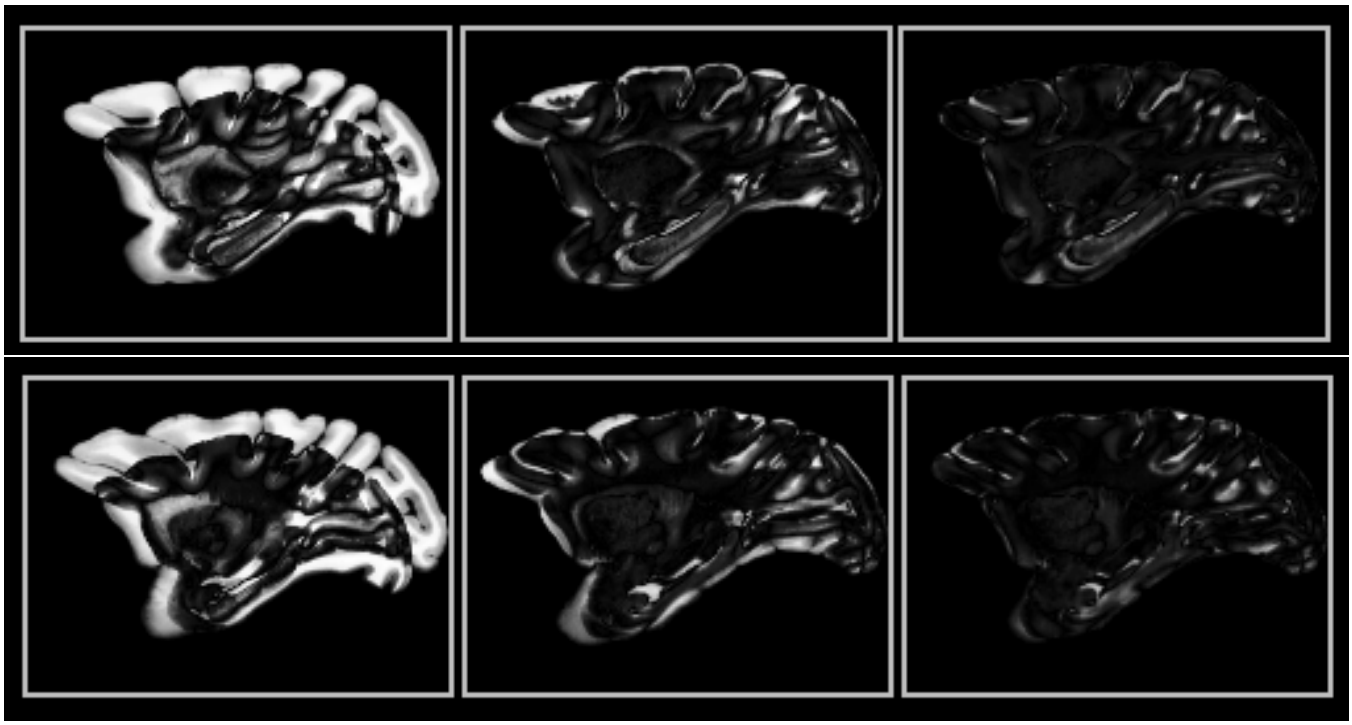

Figure 5: Magnitude difference images between the template 87A and the target 93G (left), the deformed template driven only by the sulcal maps (middle), and the volume based transformation (right).


[14] J.T. Kent and K. V. Mardia, "The link between kriging and thin-plate splines", in *Probability, Statistics and Optimisation*, F. P. Kelly, Ed. John Wiley and Sons, 1994.

[15] Grace Wahba, *Spline Models for Observational Data*, vol. Regional Conference Series in Applied Mathematics, SIAM, 1990.

[16] D.J. Felleman and D.C. Van Essen, "Distributed hierarchical processing in the primate cerebral cortex", *Cerebral Cortex*, vol. 1, no. 1, pp. 1047–3211, 1991.